

NCHRP 24-31

LRFD DESIGN SPECIFICATIONS FOR SHALLOW FOUNDATIONS

Final Report
September 2009

**APPENDIX F
SHALLOW FOUNDATIONS MODES OF FAILURE AND FAILURE
CRITERIA**

Prepared for
National Cooperative Highway Research Program
Transportation Research Board
National Research Council

LIMITED USE DOCUMENT

This Appendix is furnished only for review by members of the NCHRP project panel and is regarded as fully privileged. Dissemination of information included herein must be approved by the NCHRP and Geosciences Testing and Research, Inc.

Shailendra Amatya
Robert Muganga
Geotechnical Engineering Research Laboratory
University of Massachusetts Lowell
1 University Avenue, Lowell, MA 01854

Samuel G. Paikowsky
Geosciences Testing and Research, Inc.
55 Middlesex Street, Suite 225, North Chelmsford, MA 01863
and
Geotechnical Engineering Research Laboratory
University of Massachusetts Lowell
1 University Avenue, Lowell, MA 01854

F.1 MODES OF FAILURE FOR SHALLOW FOUNDATIONS ON SOILS

F.1.1 Overview

It is known observing the behavior of foundations subjected to load that bearing capacity occurs as a shear failure of the soil supporting the footings (Vesić, 1975). The three principal modes of shear failure under foundations are: general shear failure, local shear failure and punching shear failure.

F.1.2 General Shear Failure

General shear failure is characterized by the existence of a well-defined failure pattern consisting of a continuous slip surface from one edge of the footing to the ground surface. Unless the structure prevents the footings from rotating, the failure is also accompanied by tilting of the footing. Bulging of adjacent soil on both sides of the footing can also be seen. A schematic diagram of this failure is shown in Figure F-1. These failures are sudden, and catastrophic. The load-settlement curve shows a prominent peak, as in the schematic in Figure F-1, which means that after a certain load, the vertical displacement increases even for a lesser load than that at the peak. It may also be possible that the curve reaches the maximum load asymptotically, without a prominent peak as shown, but with a sudden clear change in its slope. Static test of a 3inch footing after failure is shown in Figure F-2. It can be observed that the slip lines have developed clearly from the edge of footing to the ground surface. When failure takes place under an eccentric vertical loading, there could occur a one-sided rupture surface as shown in Figure F-3.

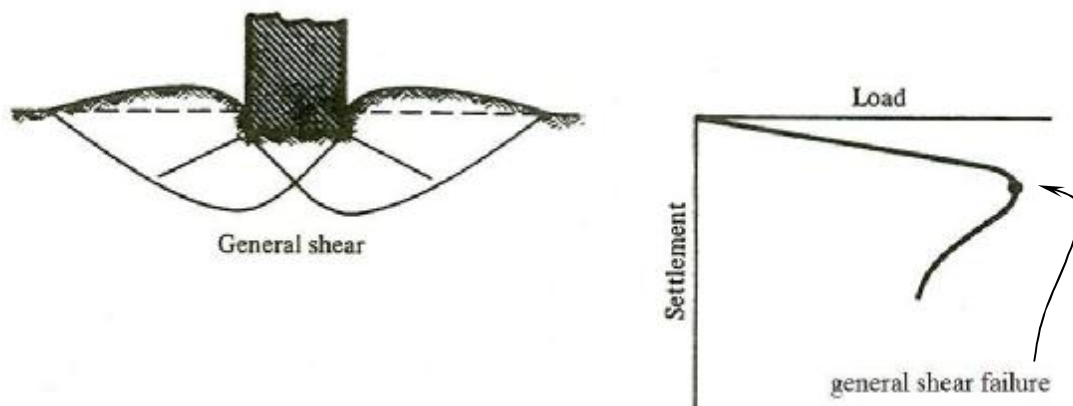


Figure F-1. Modes of bearing capacity failure: general shear failure (Vesić, 1975)

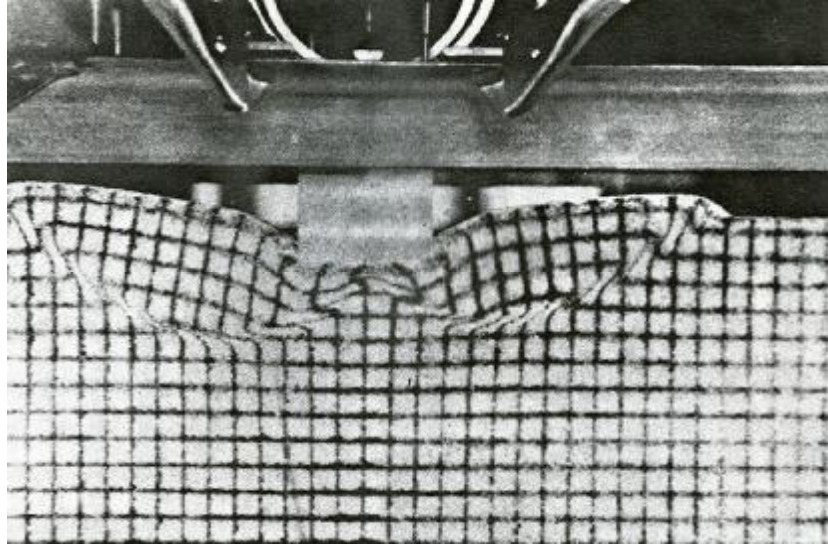


Figure F-2. Static test of a 3in footing under a centric vertical loading; the slip surfaces under the footing and its sides developed after general shear failure can be identified by the changes in the grid markers (Selig and McKee, 1961)

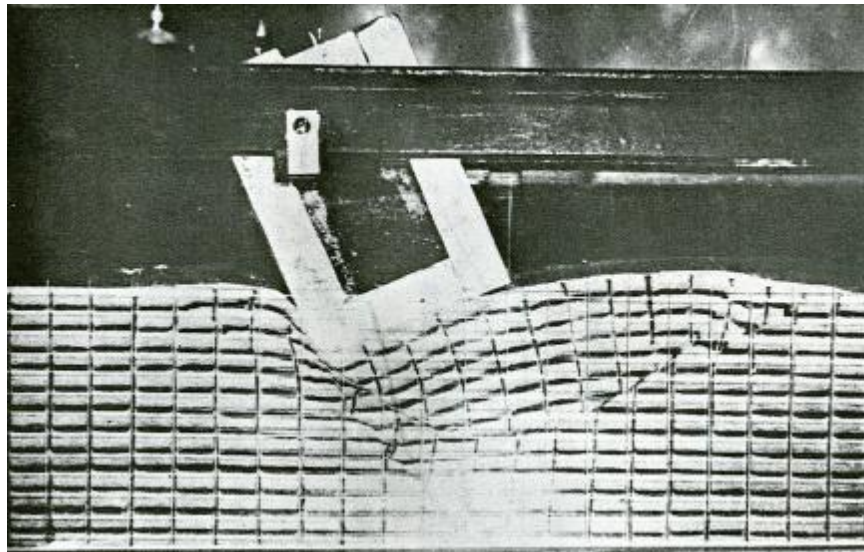


Figure F-3. One-sided rupture surface from a vertical, eccentric load (Jumikis, 1956)

F.1.3 Local Shear Failure

Local shear failure is characterized by a failure pattern clearly observable only immediately below the footing. This consists of a wedge and slip surfaces originating at the edges of the footing just as in the case of general shear failure. However, the vertical compression under the footing is significant and the slip surfaces end somewhere in the soil mass (shown by dotted lines in Figure F-4). Only after some considerable displacement of the footing, the slip surfaces appear on

the ground surface. Local shear failure retains some characteristics of both the general shear and punching modes (discussed next) of failure. When the load per unit area equals $q_{u(1)}$, the movements are accompanied by jerks. This load per unit area $q_{u(1)}$ is referred to as the first failure load (Vesić, 1963). The load-settlement curve does not show a clear peak as in the general shear failure.

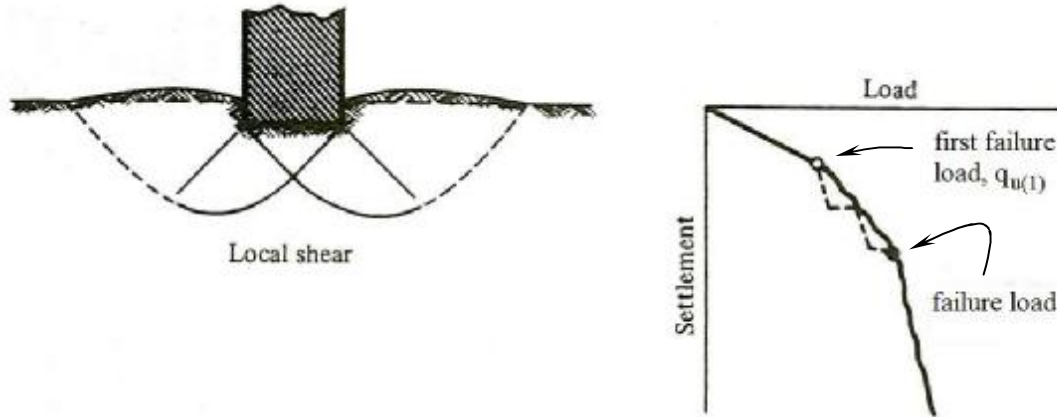


Figure F-4. Modes of bearing capacity failure: local shear failure (Vesić, 1975)

F.1.4 Punching Shear Failure

In punching shear failure, the failure pattern is not easy to observe, unlike in the failure modes discussed earlier. As the load increases, the compression of the soil immediately below the footing occurs, and the continued penetration of the footing is made possible by vertical shear around the footing perimeter. There is practically no movement of the soil on the sides of the footing, and both the horizontal and vertical equilibrium are maintained, except for the jerks or sudden movements in the vertical direction. A continuous increase in the vertical load is needed to maintain the movement in vertical direction. The schematic of soil movement and the load-settlement curves for the punching shear failure are shown in Figure F-5. These curves have steeper slopes than for those with local shear failures.

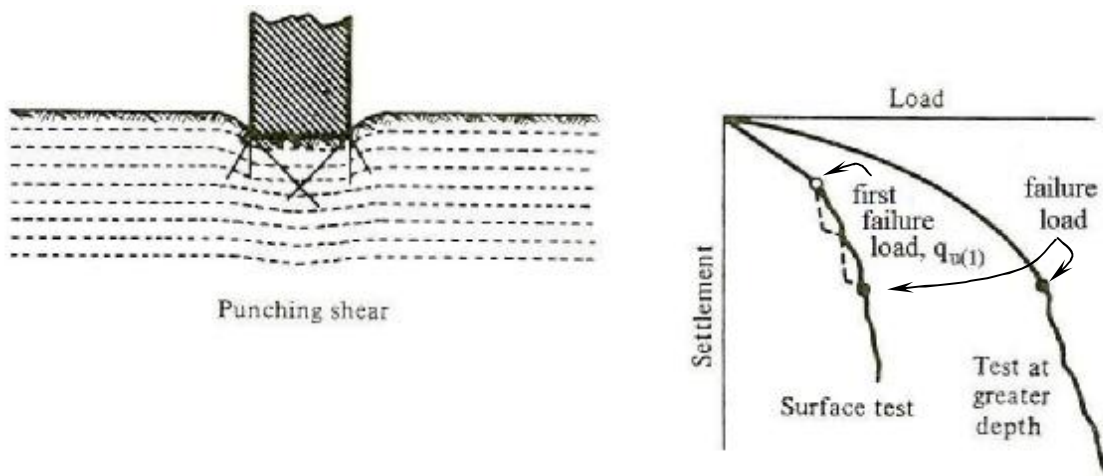


Figure F-5. Modes of bearing capacity failure: punching shear failure (Vesić, 1975)

Studies have shown that it can be generally said that if the soil is incompressible and has a finite shear strength, a footing on this soil will fail in general shear, while if the soil is very compressible, it will fail in punching shear (Vesić, 1975). When the relative density of the soil beneath the foundation is known, one can expect either of the failure modes according to the embedment depth to footing width ratio, as shown in Figure F-6. It is worthwhile to note that general shear failures are limited to relative depths of foundation (D/B^*) of about 2.0. This is the reason why Terzaghi's bearing capacity equation, and its modifications, are restricted to $D/B^* \approx 2$. Further increase in the relative depth changes the behavior of the foundation from shallow foundation to deep foundation. The slip zones develop around the foundation tip, which is significantly different from punching shear failure.

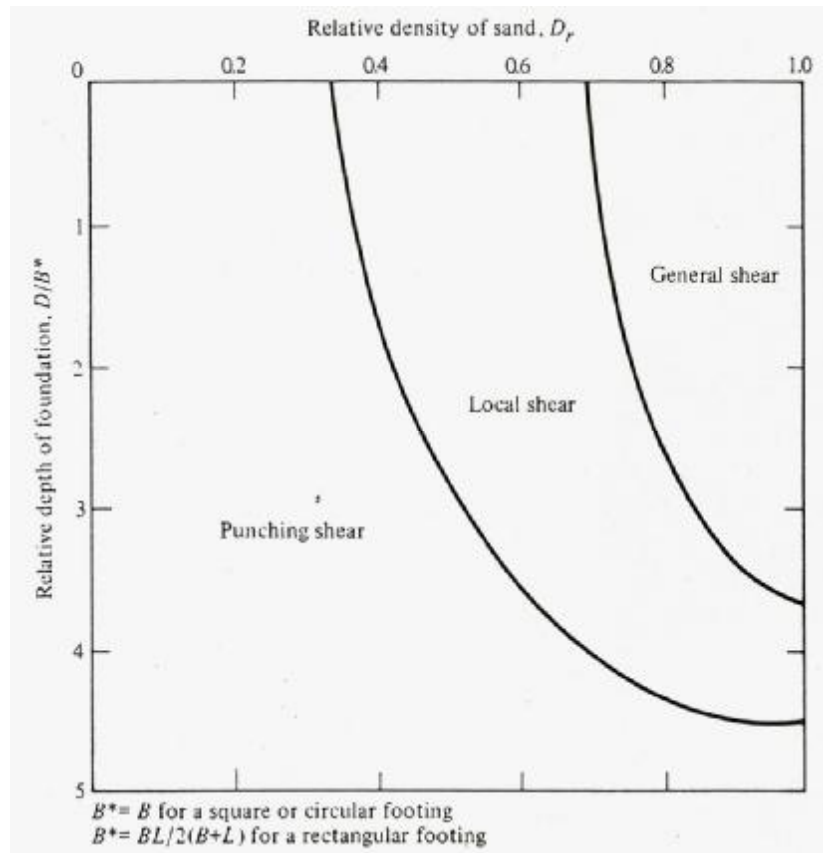


Figure F-6. Modes of failure of model footings in sand (after Vesić 1963, as modified by De Beer, 1970)

F.2 FAILURE (ULTIMATE LOAD) CRITERIA

F.2.1 Overview – Shallow Foundations on Soils

The strength limit state is “failure” load or the ultimate capacity of the foundation. The interpretation of the failure or ultimate load from a load test is made more complex by the fact that

the soil type alone does not determine the mode of failure (Vesić, 1975). For example, a footing on very dense sand can also fail in punching shear if the footing is placed at a greater depth, or if loaded by a transient, dynamic load. The same footing will also fail in punching shear if the very dense sand is underlain by a compressible stratum such as loose sand or soft clay. It is clear from the above discussion that failure load of the footing is only clearly defined for the case of general shear failure, and for the cases of the other two modes of failure, it is often difficult to establish a unique failure load. Criteria for the failure load interpretation proposed by different authors are presented in the following sections. Such interpretation requires that the load test be carried to very large displacements, which constrains the availability of test data, in particular for larger footing sizes.

F.2.2 Minimum Slope Failure (Ultimate) Load Criteria, Vesić (1963)

Based on the load-settlement curves, a versatile ultimate load criterion recommended for general use is to define the ultimate load at the point where the slope of the load-settlement curve first reaches zero or a steady, minimum value. The interpreted ultimate loads for different tests are shown as black dots in Figure F-7 for soils with different relative densities, D_r . For footings on the surface of or embedded in the soils with higher relative densities, there is a higher possibility of failure in general shear mode and the failure load can be clearly identified as for the test identified as test number 61 in Figure F-7. For footings in soils with lower relative densities however, the failure mode could be local shear or punching shear, with the identified failure location being arbitrary at times (e.g. for test number 64). A semi-log scale plot with the base pressure (or load) in logarithmic scale can be used as an alternative to the linear scale plot if it facilitates the identification of the starting of minimum slope and hence the failure load.

F.2.3 Limited Settlement Criterion of 0.1B, Vesić (1975)

For the cases in which the point of minimum slope of the curve cannot be established with certainty, Vesić (1975) suggests to adopt a limit of critical settlement, such as 10 percent of the footing width. The dotted line in Figure F-7 represents this criterion. It can be seen that this criterion is a conservative estimate for the presented tests and may become a problem for larger foundations, of say $B > 4\text{ft}$.

F.2.4 Interpretation from the Log-Log Plot of Load-Settlement Curve, De Beer (1967)

The normalized or absolute loads versus the normalized or absolute settlements are plotted in logarithmic scales. The ultimate load is defined as the change in load settlement region identified as the point of break of the load-settlement curve, as shown by the circled dots in Figure F-8. It has been found that this criterion gives very conservative interpreted failure loads for local and punching shear failures as compared to the Minimum Slope criterion.

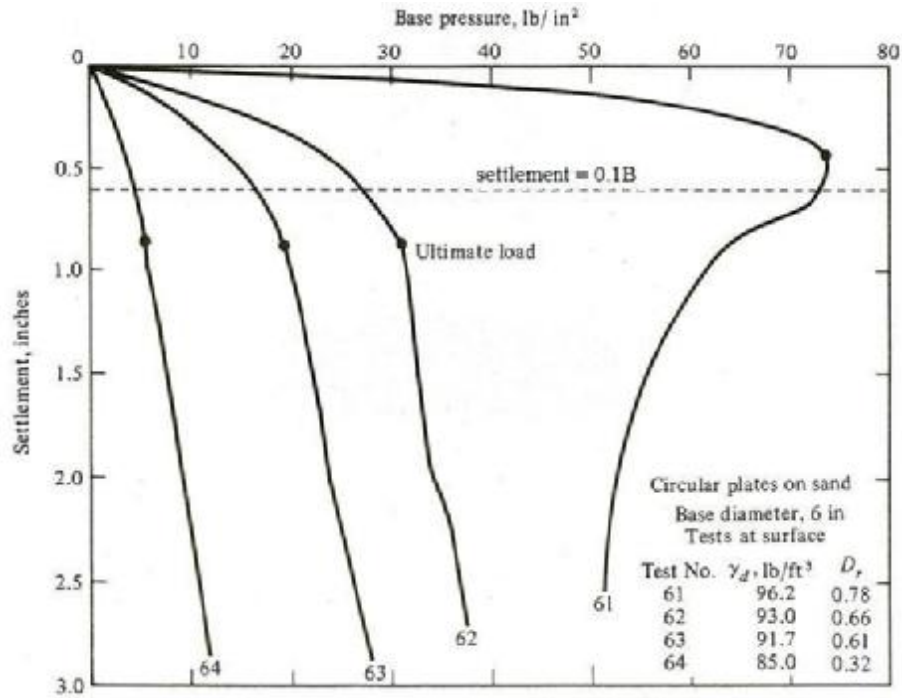


Figure F-7. Ultimate load criterion based on minimum slope of load-settlement curve (Vesić, 1963; modified to show settlement = 0.1B)

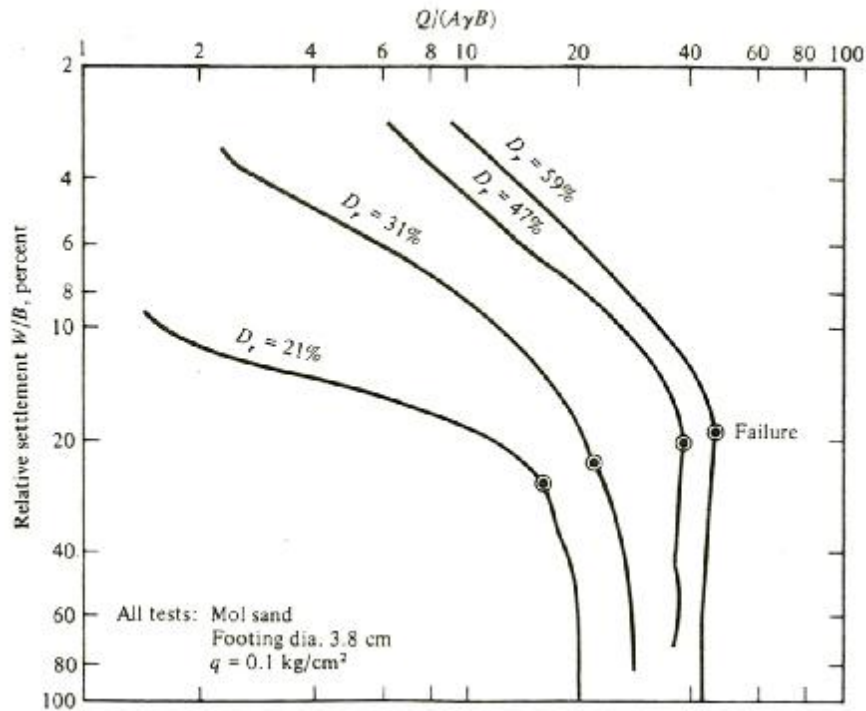


Figure F-8. Ultimate load criterion based on plot of log load versus log settlement; g is unit weight of sand, B is footing width and A is the contact area (Mol sand is from Mol, Belgium) (De Beer, 1967)

F.2.5 Two-Slope Criterion

A common variation to the Minimum Slope or De Beer's approach is the 'shape of curve' or the 'two-slope criterion' shown in Figure F-9 (e.g. NAVFAC, 1986). In this approach, the asymptotes of the load-settlement curve at the linear region at the start of loading and that towards the end of the loading are constructed in either a linear or a logarithmic scale load-settlement plot (however, for the reason stated in De Beer's approach, a linear scale plot is desirable). The pressure corresponding to the point where these asymptotes intersect is taken as the failure. There is sometimes a possibility to interpret a range of failure loads, especially when using this approach, as shown in Figure F-9. A reasonable interpretation of the failure load in such a case can be taken as the average value of the identified load range.

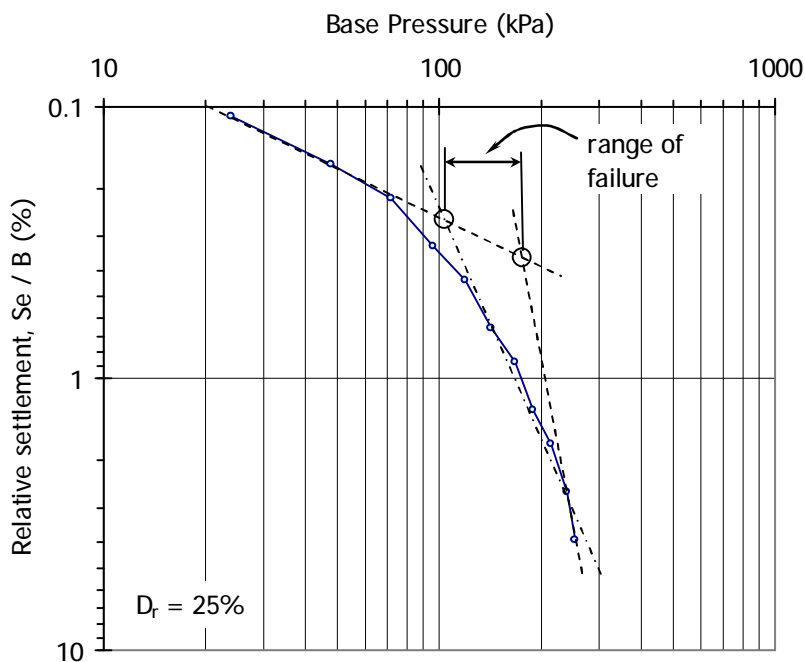


Figure F-9 Ultimate load criterion based on load-settlement curve in logarithmic scales (NAVFAC, 1986) for footing case FOTID 69 in the UML-GTR ShalFound07 database; the failure load ranges from about 100kPa to 180kPa.

F.2.6 Failure Criteria for Footings on Rock

The bearing capacity interpretation for loaded rock is complex because of the discontinuities in rock masses. Sowers (1979) mentions that for a rock mass with vertical open discontinuities, where the discontinuity spacing is less than or equal to the footing width, the likely failure mode is uniaxial compression of rock columns. For a rock mass with closely-spaced, closed discontinuities, the likely failure mode is the general wedge occurring when the rock is normally intact. For a mass with vertical open discontinuities spaced wider than the footing width, the likely failure mode is splitting of the rock mass, and is followed by a general shear failure. For the inter-

pretation of ultimate load capacities from the load-settlement curves, the L_1 - L_2 method proposed by Hirany and Kulhawy (1988) was adapted.

A typical load-displacement curve for foundations on rock is presented in Figure F-10. Initially linear elastic load-displacement relations take place, the load defining the end of this region is interpreted as Q_{L1} . If a unique peak or asymptote in the curve exists, this asymptote or peak value is defined as Q_{L2} . There is a nonlinear transition between loads Q_{L1} and Q_{L2} . If a linear region exists after the transition as in Figure F-10, the load at the starting of the final linear region is defined as Q_{L2} . In either case, Q_{L2} is the interpreted failure load.

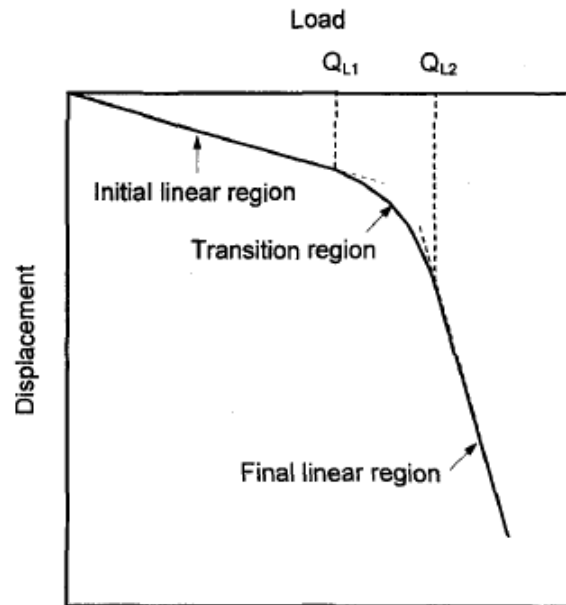


Figure F-10. Example of L_1 - L_2 method for capacity of foundations on rocks showing regions of load-displacement curve and interpreted limited loads (Hirany & Kulhawy, 1988)

F.3 SELECTED FAILURE CRITERIA

F.3.1 Foundations on/in Soils

In order to examine the different criteria and establish a preferable method for defining the bearing capacity of shallow foundations on soils, the following failure criteria were used to interpret the failure load from the load-settlement curves of footings with centric vertical loading on granular soils (measured capacity):

- (a) Minimum slope criterion (Vesić, 1963)
- (b) Limited settlement criterion of $0.1B$ (Vesić, 1975)
- (c) Log-log failure criterion (De Beer, 1967)
- (d) Two-slope criterion (shape of curve)

Examples F1 and F2 below demonstrate the application of the examined criteria to database UML/GTRShalFound07. The measured bearing capacity could be interpreted for 196 cases using

criterion (a) and 119 cases using criterion (c). Most of the footings failed before reaching a settlement of 10% of footing width (criterion (b) could therefore only be applied for 19 cases). For the selection of one failure criterion which could be recommended to be used for measured capacity interpretation from load test results, a single “representative” value of the relevant measured capacity was assigned to each footing case. This was done by taking an average of the measured capacities interpreted using criteria (a) through (d). The statistics of the ratios of this representative value over the interpreted capacity using minimum slope criterion and log-log failure criterion, were comparable with the mean of the ratio for criterion (a) being 0.98 versus that for criterion (b) being 0.99. Due to the simplicity and versatility in its application, the Minimum Slope criterion was selected as the failure interpretation criterion to be used for all cases of footing, including those with combined loadings. Figure F-11 shows the histogram for the ratio of the representative value to the interpreted capacity using minimum slope criterion. It can also be said from the figure that the measured capacity interpreted using minimum slope criterion has a slight overprediction.

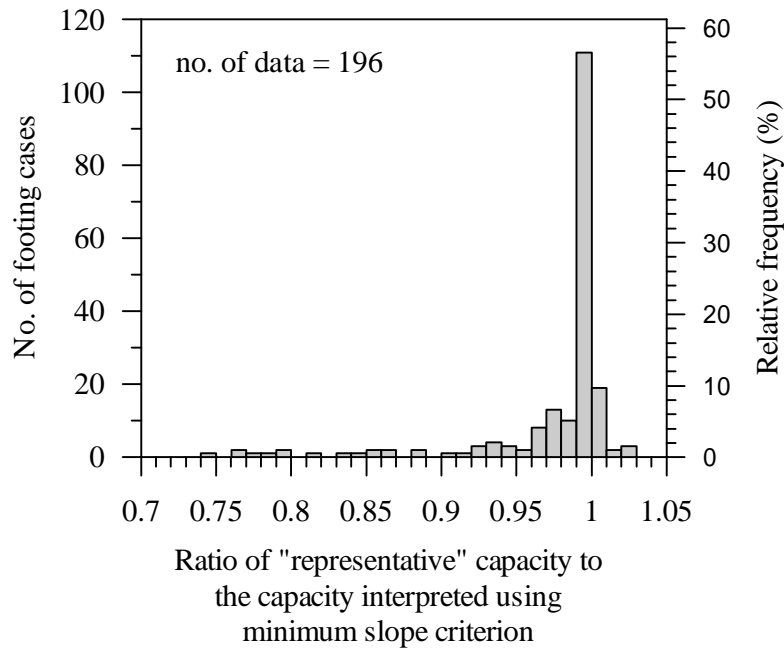


Figure F-11. Histogram for the ratio of “representative” measured capacity to the interpreted capacity using minimum slope criterion for 196 footing cases in granular soils under centric vertical loading

F.3.2 Foundations on Rocks

One failure criterion was adopted for the interpretation of the ultimate load for all foundation cases on rocks; the L_1 - L_2 method (Hirany and Kulhawy, 1988). The selection of the ultimate load using this criterion is demonstrated in Example F3 below using a footing case from the database. It can be noted that the axes aspect ratios (scales of axes relative to each other) in the plot of load-settlement curve changes the curve shape, hence could affect the interpretation of the ultimate load capacity. However, unlike for the ultimate capacity interpretation from pile load tests

which utilizes the elastic compression line of the pile, there is no generalization of what the scales of the axes should be relative to each other for the shallow foundation load tests. It can only be said that depending on the shape of the load-settlement curve, a “favorable” axes aspect ratio needs to be fixed on a case-by-case basis using judgment, such that the region of interest (e.g. while using the Minimum Slope criteria, the region where the change in the curve slope occurs) would be clear. The L_1-L_2 method was applied to all cases for which the load-settlement curve was available with sufficient detail and extent to be employed. For all other cases, the reported failure was adopted as the foundations capacity.

Example F1: Ultimate load interpretation for a footing case on granular soil from UML-GTR ShalFound07 database (medium scale footing load test)

Example FOTID #35

Title:

TEXAS A&M UNIVERSITY, RIVERSIDE CAMPUS, 1.0m x 1.0m

Reference:

Briaud, J. & Gibbens, R. (1994) "Predicted and Measured Behavior of Five Spread Footings on Sand" Geotechnical Special Publication No. 41, ASCE Specialty Conference: "Settlement '94", ASCE

Footing information:

Length, $L = 1.0\text{m} = 39\text{in}$
 Width, $B = 1.0\text{m} = 39\text{in}$
 Footing embedment, $D_f = 0.71\text{m} = 28\text{in}$
 Footing thickness = $1.17\text{m} = 46\text{in}$

Soil layer information:

Medium dense tan silty fine sand from ground level till the depth of 11.5ft (3.5m)
 Medium dense silty sand with clay and gravel between depth of 11.5ft (3.5m) to 23ft (7.0m)
 Ground water table present at 16ft (4.9m)

Average relative density of soil layer to a depth of $2B = 50.75\%$
 Average unit weight of soil to a depth of $2B = 118.38\text{pcf} (18.58\text{kN/m}^3)$
 Average relative density of soil layer to a depth of $3B = 50.4\%$
 Average unit weight of soil to a depth of $3B = 117.87\text{pcf} (18.54\text{kN/m}^3)$

Ultimate load interpretation from load-settlement curve:

With the soil information available, we can expect a local shear failure (Figure F-6) for this footing. The interpreted ultimate loads using each criterion are as follows.

Criterion (a): in Figure EF1-2, we can observe that the minimum slope starts at a load of 13.94tsf ($S_e/B = 7.8\%$). Hence, from the minimum slope criterion (Vesic, 1963), the interpreted ultimate load is 13.94tsf (1335kPa).

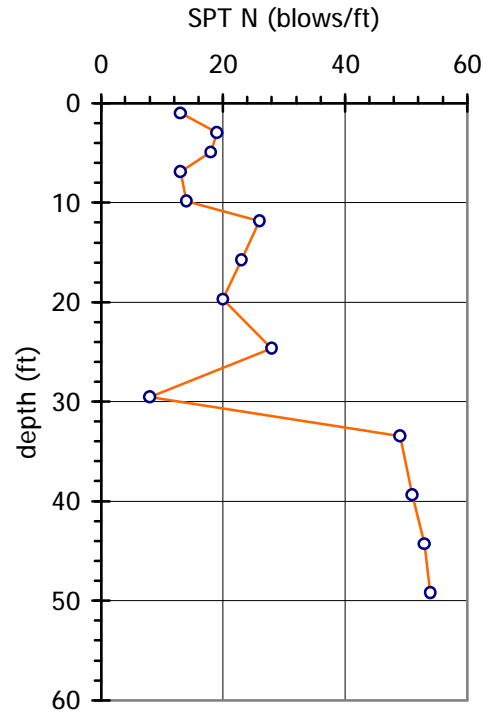


Figure EF1-1 SPT-N values at the site

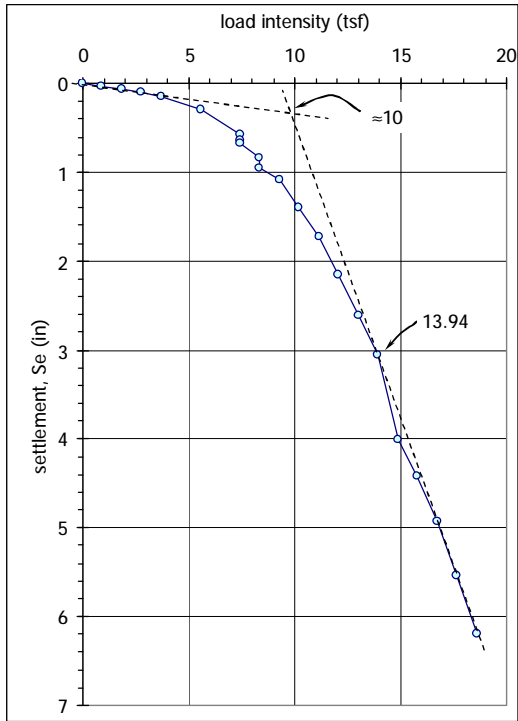


Figure EF1-2 Load-settlement curve in linear scales

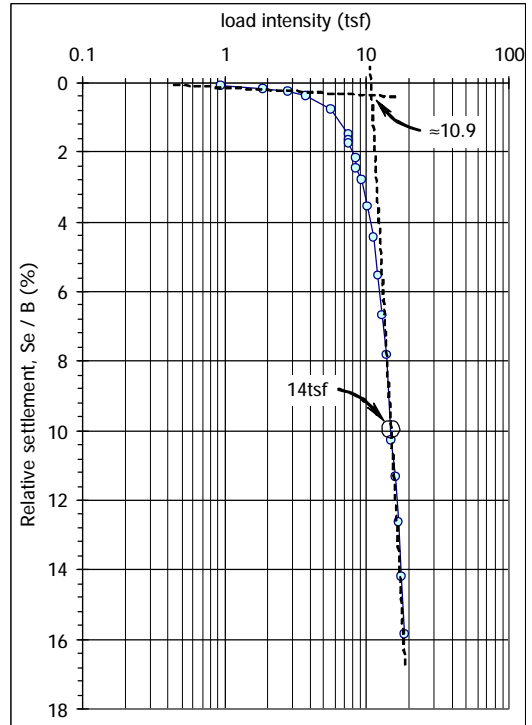


Figure EF1-3 Load-settlement curve in semi-log plot and failure load as the load at 10% relative settlement

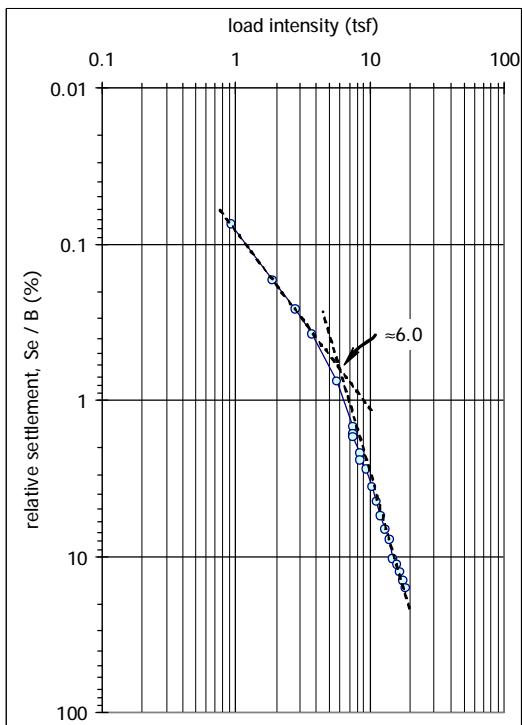


Figure EF1-4 Load-settlement curves in logarithmic scales

Criterion (b): in Figure EF1-3, the load intensity in

logarithmic scale versus relative settlement in linear scale is plotted. It can be seen that the interpreted ultimate load using $0.1B$ criterion is 14.0tsf.

Criterion (c): Figure EF1-4 is the plot in logarithmic scales. This is essentially the same as the plot in Figure F-8, with the difference being non-normalized load intensity. It can be seen that the change identified as a point of break in load-settlement region in the load-settlement curve, which is marked by a circled black dot in Figure F-8, is not clear for this footing case. Hence, it is not recommended to use De Beer's failure here.

Criterion (d): Ultimate load interpreted as the intersection of the asymptotes to the initial linear portion and the later linear portion of the curve as shown by dotted lines in the figures. The asymptotes drawn for the initial linear portion and the final linear portion of the curve, shown by dotted lines in Figure EF1-2, the failure load at the intersection is 10tsf. From the semi-log plot in Figure EF1-3, the failure load interpreted at the intersection of the asymptotes is 10.9tsf. The failure load interpretation as shown in Figure EF1-4 is mentioned in NAVFAC (1986); the asymptotes intersect at 6.0tsf. This is very conservative compared to the failure loads obtained from linear and semi-log scale plots.

The ultimate load:

It is seen that a multiple interpretation of the ultimate load is possible for the same load-settlement curve. For the reasons of simplicity and versatility as stated in the previous section, the failure load interpreted using minimum slope criterion by Vesic (1963) is taken as the ultimate load, which is 13.94tsf (1335kPa).

Example F2: Ultimate load interpretation for a footing case on granular soil from UML-GTR ShalFound07 database (small scale footing load test)

Example FOTID #371 (PeA1.59)

Title:

Small scale model test 0.09 x 0.09 m

References:

- (1) Perau (1995) "Ein systematischer Ansatz zur Berechnung des Grundbruchwiderstands von Fundamenten" Mitteilungen aus dem Fachgebiet Grundbau und Bodenmechanik, Heft 19 der Universitaet Essen, edited by Prof. Dr.-Ing. W. Richwien (in German)
- (2) Perau (1997) "Bearing Capacity of Shallow Foundations" Soils and Foundations Vol. 37, No. 4, 77-83

Footing information:

$L = 0.09\text{m} = 3.54\text{in}$
 $B = 0.09\text{m} = 3.54\text{in}$
 $D_f = 0.0\text{in}$

Soil layer information:

Dense to very dense medium to coarse sand to the depth of 5.9in (0.15m)
 Groundwater not present
 Relative density of soil $D_r = 90.1\%$
 Unit weight of soil = 110.5pcf (17.34kN/m³)

The ultimate load:

The mode of failure for this test lies in the general failure zone ($D_r > 67\%$). The interpreted ultimate load from Figure EF2-1, using Criterion (a) is 2.63tsf (251.6kPa). In this example, interpretation using relative settlement of 10% (Criterion (b)) does not work, as the failure occurs at a ratio well below 10%. Changing the axes aspect ratio in Figure EF2-3 (as compared to Figures EF2-1 and EF2-2) and using Criterion (c), an ultimate load of about the same magnitude as that obtained using Criterion (a) is obtained. This ultimate load cannot be clearly identified using Figure EF2-3 alone. Hence, it is beneficial to compare curves plotted in different scales as well as axes aspect ratios.

The two-slope criterion (Criterion (d)) results with a conservative estimation of failure load as compared to that obtained using Criterion (a): 2.43tsf in linear scale plot and 1.93tsf in semi-log scale plot respectively.

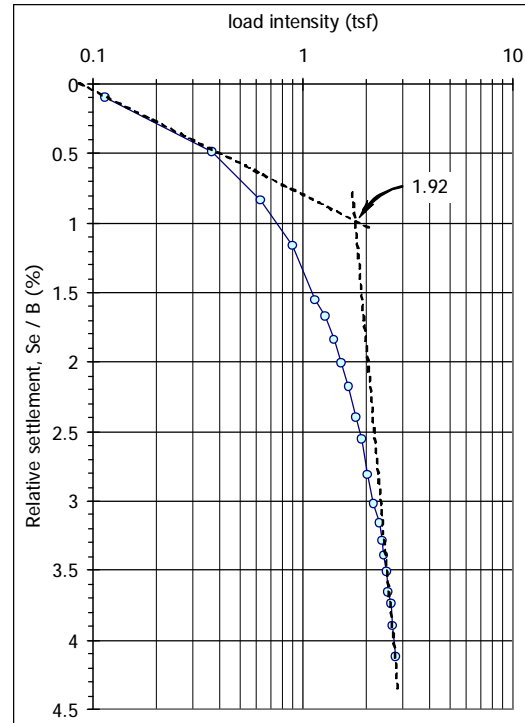


Figure E2-2 Load-settlement curves in semi-log scales

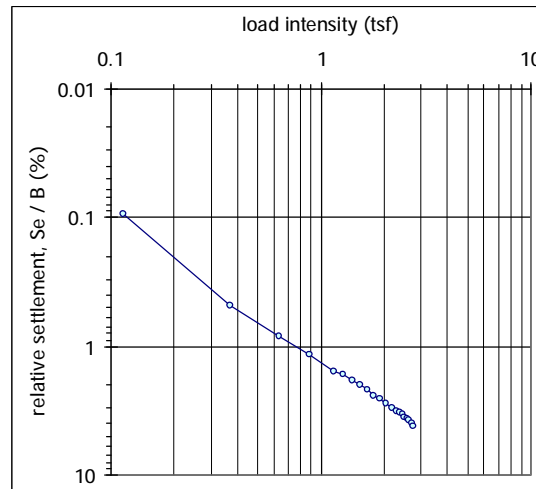


Figure E2-3 Load-settlement curves in logarithmic scales

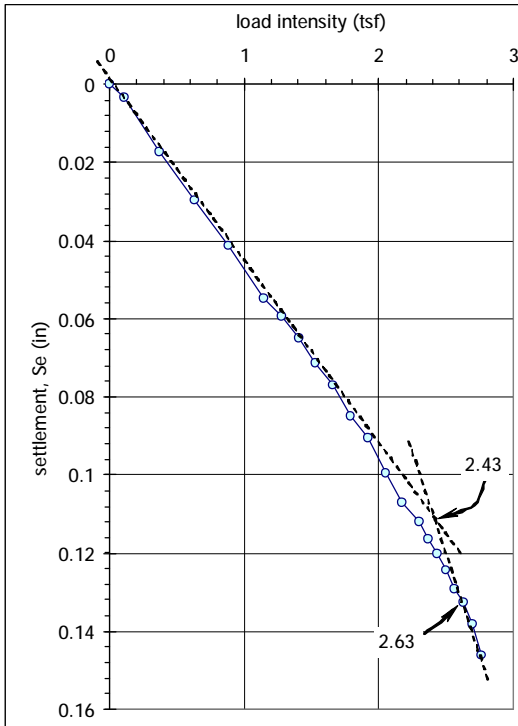


Figure E2-1 Load-settlement curves in linear scales

Example F3: Ultimate load interpretation for a footing case on rock from UML-GTR RockFound07 database

FOOTING CASE # 69

Reference:

Orpwood, T.G., Shaheen, A.A. & Kenneth, R.P (1989) "Pressuremeter evaluation of glacial till bearing capacity in Toronto, Canada" Foundation Engineering: Current Principles and Practices, ed. F.H. Kulhawy, Vol.1, pp.16-28; ASCE, Reston: Virginia

Footing information:

Circular footing of 2.5ft diameter

Rock information:

Rock type: Till; till has a uniaxial compressive strength comparable to a rock
Discontinuity spacing: fractured
Uniaxial compressive strength = 16.92ksf (number of tests = 1)

Ultimate load interpretation from load-settlement curve:

In Figure EF3-1, the load-settlement curve for the footing shows clear initial and final linear regions. The interpreted ultimate load is defined by Q_{L2} , which is the starting of the final linear region of the curve, and is equal to 43.33tsf (86.67ksf).

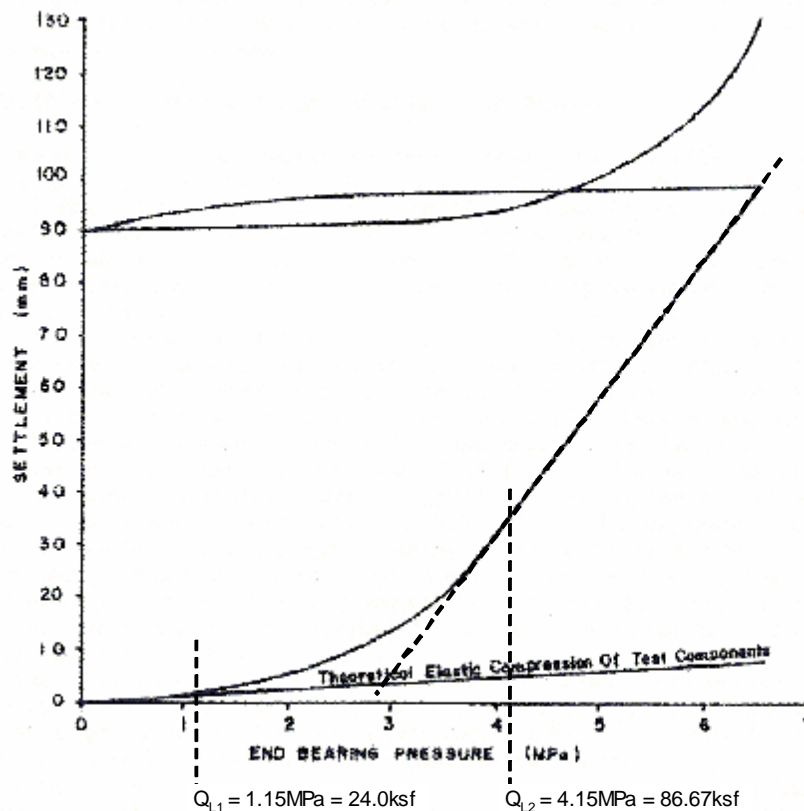


Figure EF3-1. Load-settlement curve and the interpreted failure load, $Q_{L2} = 86.67 \text{ ksf}$

REFERENCES

- Briaud, J. and Gibbens, R. (1994). "Predicted and Measured Behavior of Five Spread Footings on Sand" Geotechnical Special Publication No. 41, ASCE Specialty Conference: *Settlement '94*, ASCE.
- De Beer, E.E. (1967) *Proefondervindelijke bijdrage tot de studie van het gransdragvermogen van zand onder funderingen op staal; Bepaling von der vormfactor sb*, Annales des Travaux Plublics de Belgique, 68, No.6, pp.481-506; 69, No.1, pp.41-88; No.4, pp.321-360; No.5, pp.395-442; No.6, pp.495-522
- Hirany, A. and Kulhawy, F.H. (1988) *Conduct and Interpretation of Load Tests on Drilled Shaft Foundation: Detailed Guidelines*, Report EL-5915 (1), Electric Power Research Institute, Palo Alto, Jul 1988, 374 p
- Jumikis, A.R. (1956) *Rupture surfaces in sand under oblique loads*, J. of Soil Mechanics and Foundation Design, ASCE, Vol.82, No.SM 1
- Naval Facilities Engineering Command Design Manual 7.01 (NAVFAC) (1986)
- Orpwood, T.G., Shaheen, A.A. and Kenneth, R.P (1989). "Pressuremeter evaluation of glacial till bearing capacity in Toronto, Canada" *Foundation Engineering: Current Principles and Practices*, ed. F.H. Kulhawy, Vol.1, pp.16-28; ASCE, Reston: Virginia.
- Perau (1995) "Ein systematischer Ansatz zur Berechnung des Grundbruchwiderstands von Fundamenten" *Mitteilungen aus dem Fachgebiet Grundbau und Bodenmechanik*, Heft 19 der Universitaet Essen, edited by Prof. Dr.-Ing. W. Richwien (in German).
- Perau (1997) "Bearing Capacity of Shallow Foundations" *Soils and Foundations* Vol. 37, No. 4, 77-83.
- Selig, E.T. and McKee, K.E. (1961) *Static behavior of small footings*, J. of Soil Mechanics and Foundation Design, ASCE, Vol.87, No.SM 6
- Sower, G.F. (1979) *Introductory soil mechanics and foundations*, 4th ed, Macmillan Publishing: New York
- Vesic, A. (1963) *Bearing capacity of deep foundations in sand*, Highway Research Record, 39, National Academy of Sciences, National Research Council, pp.112-153
- Vesić, A. (1975). "Bearing Capacity of Shallow Foundations", *Foundation Engineering Handbook* (eds. H.F. Winterkorn and H.Y. Fang), Van Nostrand Reinhold, New York, pp.121-147.